A Novel Look into Digital Beamforming Techniques for Multipath and Interference Mitigation in Galileo Ground Stations

Jose Lopez Vicario[1], Marc Barcelo[1], Marti Mañosas[1], Gonzalo Seco-Granados[1],
Felix Antreich[2], Joan Manuel Cebrian[3], Joan Picanyol[3] and Francisco Amarillo[4]
[1] SPCOMNAV - Universitat Autonoma de Barcelona (UAB), [2] German Aerospace Center (DLR),
[3] Indra Espacio, [4] European Space Agency (ESA)

***Abstract*—In this paper, we explore the adoption of Array Signal Processing in Galileo Ground Stations. The main motivation comes from the need of efficiently mitigating multipath and interference sources in order to achieve centimetre accuracy. One of the critical aspects appearing when an array of antennas is implemented resides on the array perturbations and mismodelling. For that reason, this work places special emphasis on this issue and some robust beamforming techniques are proposed. Differently from other studies addressing the use of conventional beamforming techniques for navigation applications, we propose novel strategies specially adapted to the considered scenario. As shown in the paper, the use of digital beamforming allows for a (at least) 47% reduction in terms of tracking errors when compared to a single antenna receiver.**

I. Introduction

Navigation accuracy demanded by the under development Galileo system motivates the study and design of advanced receiving techniques. In the context of the Galileo Ground Mission Segment, high performance tracking stations achieving centimetre level tracking accuracy are required to provide the system with accurate satellite ephemeris and clock prediction models [1]. Tracking stations work in static and controlled scenarios, being the ionospheric perturbations, multipath and interference components the dominant error sources. One of the most promising approaches to cope with multipath and interference signals is the adoption of arrays of antennas at the ground station receivers [2], [3]. Besides, the array gain provided by such kind of solution also alleviates the signal power loss induced by ionospheric fading.

The main problem arising when an antenna array is implemented in practice, however, is the extreme difficult to perfectly control and calibrate all the components of the system. Typical array perturbations are due to the non-ideal response of the hardware elements (antenna and RF chains), mutual coupling effects, cross-polarization coupling and antenna position errors, etc. Indeed, the array performance is quite sensitive to these perturbations, showing dramatic performance losses if these are not carefully addressed. For that reason, this paper gives special emphasis to this issue by considering different perturbation sources and proposing robust digital beamforming techiques to cope with them.

Concerning the digital beamforming solutions, some misconceptions drive the designers to propose non-adequate solutions such as the well-known Capon and MMSE beamformers [4]. These solutions are useful for communication systems but some problems appear when these are applied on the navigation context. On the one hand, the Capon solution is quite sensitive to multipath (coherent) components as the beamformer compensates all the contributions in order to minimize total output power (i.e., line-of-sight signal (LOSS) signal is cancelled). MMSE beamformer, on the other hand, tends to (constructively) combine the multipath components with the signal of interest. As a consequence, the propagation delay of the LOSS signal cannot be accurately obtained.

In this work, however, we propose novel beamforming solutions. First, a deterministic approach based on an iterative procedure is presented. This solution provides an efficient way to tailor the beampattern to specific scenarios. Besides, two adaptive beamformers are proposed. These adaptive beamformers are designed with the aim of addressing the presence of multipath components and array perturbations. The first one is based on the conventional Linearly Constrained Minimum Variance (LCMV) beamformer but, however, the solution is oriented to suppress a given space region associated to the multipath directions of arrival (DOA). The second beamformer follows the Iterative Adaptive Approach (IAA) presented in [5]. Differently from other adaptive beamformers presented in the literature, this approach provides a robust beamformer being able to efficiently managing coherent signals. In order to verify the proposed solutions, performance results in terms of tracking errors of the GNSS receiver are compared with those of a baseline case consisting in a single antenna receiver. As shown in the paper, tracking errors can be reduced at least 47% (up to 97%) when digital beamforming is considered.

[0]The work reported in this article has been supported under a contract of the European Space Agency (ADIBEAM AO/1-5934/08/NL/AT).The views presented in the paper represent solely the opinion of the authors and should be considered as R&D results not necessarily impacting the EGNOS and Galileo system design. The work of the UAB members has been also supported by the Spanish Government under project TEC2008-06305, the Catalan Government under grant 2009 SGR 298, and the Chair of Knowledge and Technology Transfer Parc de Recerca UAB - Santander. J.L. Vicario and G. Seco-Granados are also affiliated with IEEC-UAB.

II. System Model

In this work, we consider the design of the GNSS receiver for Galileo Reference Ground Stations. The main objective of such design is to achieve cm and mm accuracy for both the DLL and PLL tracking. In particular, we focus on achieving such requirements by tracking Safety-of-Life signals (pilots on L1 and E5b). Since the main sources of errors in such scenario are ionospheric scintillation, multipath and interference, we introduce the use of an array of antennas at the receiver. Next, we present some aspects of the proposed scenario and receiver design in detail.

A. Scenario Assumptions

In this work, we assume the following assumptions for the proposed scenario:

- As1: the ionospheric conditions correspond to a Sun Spot number equal to 140.
- As2: the direction-of-arrival (DOA) of the LOSS is perfectly known at the receiver.
- As3: the multipath and interference signals can only arrive with elevations equal or lower than 7.5°.

B. Antenna Array and Digital Beamforming Architecture

An overview of the general architecture of the GNSS receiver and the implementation of the digital beamforming is depicted in Figure 1. The design is following the approach of so-called post-correlation beamforming, i.e., digital beamforming is applied to digital samples at the output of the bank of correlators. This solution provides a good trade-off in terms of flexibility and complexity. This is because post-correlation allows implementing different beamforming algorithms in a flexible manner by adopting a software implementation and the beamforming weights have to be applied for much smaller rates than for pre-correlation beamforming implementation. Besides, it can be easily shown that the complexity of both pre-correlation and post-correlation beamforming is of the same magnitude.

By adopting the post-correlation solution, we need a different digital beamformer for each satellite and frequency band. In order to provide a clear picture of the proposed solution, we have restricted the architecture representation to cover only one of these digital beamformers. Indeed, we also consider such restriction in the sequel (especially in the signal modelling and beamformers description) for the ease of notation.

Concerning the antenna array configuration, we consider an M antennas uniform rectangular array (URA). The motivation of such option comes from the fact that this is a practical and feasible solution for practical implementation (reproducibility of antenna conditions, ease of calibration and manufacturing, etc.). Indeed, URA is adopted by many applications and systems for radar, sonar and communications. In this work in particular we consider a 6x6 antenna deployment where antenna separation is equal to $d = \lambda_{L1}/2$ (95 mm).

As previously commented, we propose different digital beamforming algorithms (deterministic and adaptive). Further

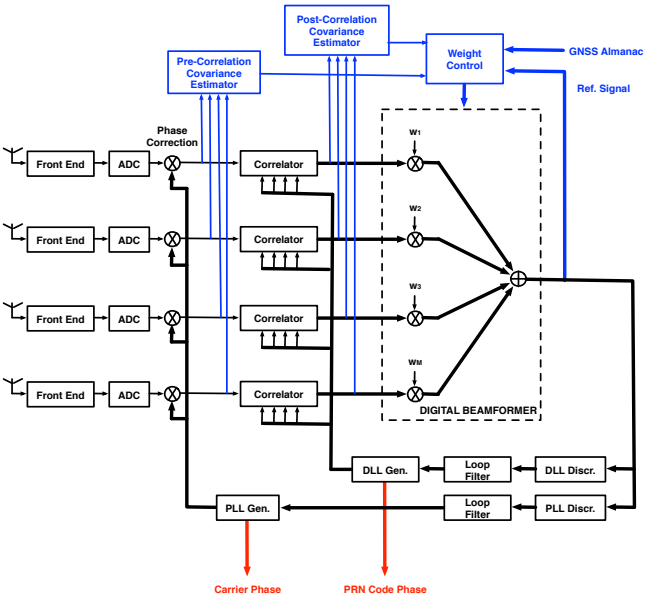

Fig. 1. Receiver Architecture based on Antenna Array.

details will be provided in the next section but, however, it is worth pointing out here that adaptation of adaptive solutions will be based on the covariance measurements at pre- and/or post-correlation levels. Thus, the spatial covariance matrix needs to be estimated pre- or post-correlation and to be introduced to the beamforming algorithms (as observed Figure 1). An estimate of the spatial covariance matrix at the pre-correlation level can be considered as an estimate of the noise-plus-interference spatial covariance matrix.

C. Signal Model

The pre-correlation digital samples of the received signal at the input of the bank of correlators (see Figure 1) can be characterized with the following $Mx1$ vector:

$$\begin{aligned}\mathbf{x}_{pre}(n) &= s_{pre}(n)\mathbf{v}_{LOSS} \\ &+ \sum_{k=1}^{N_{MP}} s_{pre}\left(n - \lfloor T_{MP_k} F_{s,pre} \rfloor\right)\mathbf{v}_{MP_k} \\ &+ \sum_{k=1}^{N_I} i_k(n)\mathbf{v}_{I_k} + \mathbf{w}(n) \end{aligned} \quad (1)$$

where $s_{pre}(n)$ stands for the Galileo signal, T_{MP_k} is the time delay of the k-th multipath component, $F_{s,pre}$ is the pre-correlation sampling frequency, i_k is the k-th interference component and $\mathbf{w}(n)$ is additive white Gaussian noise. Concerning $\mathbf{v}_{LOSS}$, $\mathbf{v}_{MP_k}$ and $\mathbf{v}_{I_k}$, these are the steering vectors corresponding to the LOSS signal, the k-th multipath component and the k-th interference component, respectively.

In the case of the signal at the output of the bank of correlators, the following expression can be adopted:

$$\mathbf{x}_{post}(n) = s_{post}(n)\mathbf{v}_{LOSS} + \sum_{k=1}^{N_{MP}} s_{post}\left(n - \lfloor T_{MP_k} F_{s,post} \rfloor\right)\mathbf{v}_{MP_k} + \sum_{k=1}^{N_I} i_k(n)\mathbf{v}_{I_k} + \mathbf{w}_{post}(n) \quad (2)$$

where $F_{s,post}$ is the post-correlation sampling frequency whereas $s_{post}(n)$, $i_{post,k}(n)$ and $\mathbf{w}_{post}(n)$ stand for the Galileo signal, the k-th interference component and the noise contribution at the output of the correlators, respectively.

As observed in Figure 1, the beamformer is applied at the output of the correlators as we adopt a post-correlation beamformer. In particular, the beamforming vector is denoted by the $Mx1$ vector $\mathbf{w}(n)$ and the beamforming operation is given by the following expression:

$$y(n) = \mathbf{w}^H(n)\mathbf{x}_{post}(n)$$

Once the beamforming output is calculated, this is fed to the tracking loops of the GNSS receiver.

As previously commented, pre-correlation and post-correlation covariance estimates have to be provided to the weight control unit in accordance with the proposed beamforming solution. The pre-correlation covariance estimate can be considered as an estimate of the spatial noise-plus-interference covariance matrix because the satellite signals and the multipath signals are of very low power and are deeply buried under the noise floor. In this work, we consider the maximum likelihood estimate of the covariance matrix, which is given in case of pre-correlation covariance by [4]:

$$\hat{\mathbf{R}}_{x,pre} = \frac{1}{K}\sum_{k=0}^{K-1} \mathbf{x}_{pre}(n-k)\mathbf{x}_{pre}^H(n-k)$$

or in case of the post-correlation covariance:

$$\hat{\mathbf{R}}_{x,post} = \frac{1}{K}\sum_{k=0}^{K-1} \mathbf{x}_{post}(n-k)\mathbf{x}_{post}^H(n-k)$$

Concerning K, this is the number of snapshots considered for estimation of the pre- and post-correlation covariance matrices. In both cases, we have considered a total number of 1000 snapshots.

Finally, we conclude this section by describing the steering modelling considered in this work. Here, it is assumed that the transmission medium between the transmitter, receiver and possible scatterers is linear, non-dispersive, and isotropic such that the radiation impinging on an array of passive sensor elements can be modeled as a superposition of wavefronts generated by point sources. The point sources are located far from the array such that the direction of propagation is nearly equal at each sensor and the wavefronts are approximately planar (far-field approximation). Thus, the propagation field within the array aperture consists of plane waves. On the other hand, we also assume that the received signals are so called narrowband (array narrowband assumption, i.e., the bandwidth of the signal is much lower than the carrier frequency) as their amplitudes and phases vary slowly with respect to the propagation time across the array. This allows the time delay of the signals across the array to be modelled as a simple phase shift of the carrier frequency while the bandwidth of the signal is concentrated around the carrier frequency. With these assumptions in mind, the Mx1 steering vector for the LOSS signal can be modelled as follows [4]:

$$\mathbf{v}_{LOSS} = \begin{bmatrix} 1 \\ e^{-\mathrm{j}\frac{2\pi d}{\lambda}\cos\theta\cos\phi} \\ \cdots \\ \mathrm{e}^{-\mathrm{j}\frac{2\pi d}{\lambda}(\cos\theta\cos\phi+\cos\theta\sin\phi)} \\ \cdots \\ \mathrm{e}^{-\mathrm{j}\frac{2\pi d}{\lambda}(\sqrt{M}-1)(\cos\theta\cos\phi+\cos\theta\sin\phi)} \end{bmatrix} \quad (3)$$

where λ is the carrier wavelength and θ and ϕ are the elevation and azimuth (expressed in radians) of the LOSS signal, respectively. In the case of the interference and multipath components, the steering vectors are identically computed by taking into account their associated elevation and azimuth angles. This expression takes into account the theoretical modeling of steering vectors. Real steering vectors, however, usually differ from the theoretical ones due to some perturbations found in practice. For that reason, we deal with the modeling of real steering vectors in the following subsection.

D. Perturbation Modelling

The main problem arising when an antenna array is implemented in practice is the extreme difficulty to perfectly control and calibrate all the components of the system. Typical array perturbations are the non-ideal response of the hardware elements (antenna and RF chains) and mutual coupling effects. For that reason, in this work we model the steering vector by considering these phenomena.

By departing from the steering vector expression presented in the previous subsection, we define a nominal steering vector $\mathbf{v}^n$, for which the m-th element can be written as follows:

$$v_{m}^{n} = g_{m}^{n}\exp\left[j\phi_{m}^{n}\right]$$

where g_{m}^{n} is the nominal gain introduced by the m-th antenna (depending on the DOA of the impinging signal) and its associated RF chain. The term ϕ_{m}^{n} is the combination of the phase delay of the impinging signal (as described in (3)) and the phase delay introduced by the hardware associated to the m-th antenna. Due to the non-idealities of the real system, the actual steering vector differs from the nominal one as follows:

$$\begin{aligned} v_{m}^{pert} &= \left(g_{m}^{n} + \Delta g_{m}\right)\exp\left[j(\phi_{m}^{n} + \Delta\phi_{m})\right] \\ &= g_{m}^{n}\exp\left[j\phi_{m}^{n}\right]\left(1 + \frac{\Delta g_{m}}{g_{m}^{n}}\right)\exp\left[j\Delta\phi_{m}\right] \\ &= v_{m}^{n}\beta_{m} \end{aligned}$$

As observed in the previous expression, each element of the steering vector is multiplied by a perturbation factor $\beta_m = \left(1 + \frac{\Delta g_m}{g_m^n}\right)\exp\left[j\Delta\phi_m\right]$. In this work, we model the

perturbation at each element as an i.i.d random variable with uniform distribution. More specifically, the gain and the phase of β_m are independently generated at each element as:

$$\left(1+\frac{\Delta g_m}{g_m^n}\right) \sim U\ \left(10^{(-P_{gain}/10)}-1, 10^{(P_{gain}/10)}-1\right)$$
$$\Delta\varphi_m \sim U\ \ (-P_{phase}\pi/180, P_{phase}\pi/180)$$

where different values have been considered for P_{gain} and P_{phase} (ranging from 0 dB and 0° to 1 dB and 1°).

Once the perturbation errors are modelled, the coupling effect is included as well. To do so, we introduce a matrix characterizing the coupling effects, $\mathbf{C}_{coup}$, as follows:

$$\mathbf{v}^{real} = \mathbf{C}_{coup}\mathbf{v}^{pert}$$

Expressions derived above are introduced in (1) and (2) to properly characterize the received signal. By considering the DOAs of the different components of the received signal, one can easily introduce the different steering vectors.

Concerning the beamforming design, we also include some information of the hardware components (such as the measured gains, phase responses and coupling effects) to model the steering vectors. More specifically, the steering vector considered in the beamformer design is given by the following expression:

$$\mathbf{v}^{design} = \mathbf{C}_{coup}\mathbf{v}^{n}$$

Notice that we avoid the inclusion of perturbations in this case as these are unpredictable. Besides, it is also worth commenting that the calibration of mutual coupling effects is not considered at digital level. The coupling matrix is measured in advance and considered for correction in the beamforming algorithm.

E. GNSS Receiver

The proposed GNSS receiver architecture is also presented in Figure 1 and can be summarized as follows:

- Tight integration with the beamformer where:
  1) Code correlators are placed before the beamfoming module (with the same frequency correction and time reference for all the antennas).
  2) Tracking loops are placed at the output of the beamforming module.
- Adoption of conventional acquisition and tracking blocks. As for the tracking blocks, the following DLL and PLL blocks are considered:
  1) A first order dot-product DLL with E-L spacing equal to 0.1 chips and bandwidth equal to 0.2 Hz.
  2) A second order arctangent PLL with bandwidth equal to 3 Hz.

The justification from such design solution is based on two premises:

- A tight integration with the beamformer is necessary in order to fully exploit the advantages of a multi-antenna receiver. That is to say, the beamformer and the receiver cannot be considered as independent units. Although this would have the benefit that a conventional receiver could be used, there would be serious performance limitations as only very simplistic pre-correlation beamformer would be possible.
- In spite of the tight integration, it is desired to build the receiver using the blocks usually found in conventional receivers, without changing their implementation, only their number and arrangement. The optimization of these blocks, such as the correlators and the tracking loops, has been carried out with great detail by the manufacturers. The fact that the design of such blocks need not be changed would pave the way for the adoption of antenna array technology by GNSS receiver manufacturers.

Concerning the parameters selected for the tracking loops, such selection is aimed at achieving low tracking errors. In other words, since the considered scenario is static, we focus the DLL design on the use of a solution oriented to the noise reduction in order to minimize tracking errors as much as possible. Concerning the PLL, we use the optimal arctangent solution because the reference stations are not complexity limited. Concerning the PLL bandwidth selection, the choice is aimed at alleviating scintillation effects. As reflected in some papers addressing ionosphere scintillation effects [6] (and references therein), the considered PLL bandwidth usually takes values between 1 and 10 Hz. In this work, we consider a value of 3 Hz in order to attain a good trade-off in terms of noise reduction vs. tracking of the carrier phase scintillation.

III. Digital Beamforming Solutions

One of the main problems of the proposed scenario is the presence of multipath signals. Most of adaptive beamforming techniques fail when incoming signals are coherent or correlated. For that reason, we first propose a deterministic beamfomer aimed at cancelling the entire interference and multipath region. Furthermore, we also propose two adaptive beamformers showing a robust behaviour against coherent signals.

A. DET: Deterministic Beamformer

Among the set of deterministic approaches, the most popular designs are based on conventional beamformers pointing to the direction the interest and the application of spectral weighting in order to reduce the sidelobe level response (see [4] for further details). After comparing different weighting schemes (uniform, discrete prolate spheroidal sequences, raised cosine, Kaiser, cosine weighting, Blackman-Harris and Dolph-Chebychev), one can clearly conclude that the best performance is obtained with Dolph-Chebychev weighting. However, due to the particularities of the considered scenario (attenuation of the pattern should be assured in a specific region, i.e., elevations lower than 7.5°), we have considered a deterministic approach that allows the design of desired pattern responses [7]. This scheme is based on an iterative approach and, as we will show later, better results than that obtained with Dolph-Chebychev can be achieved.

The design procedure of DET beamformer starts by defining the specification of the desired pattern. To do so, we define three parameters: the DOA of the LOSS signal (θ_d and ϕ_d), the sidelobe region of interest (Ω) and the desired response level at this region (ε). With this information in mind the algorithm is initialized as follows:

$$\begin{aligned} &\min_{\mathbf{w}} \mathbf{w}^H \mathbf{A} \mathbf{w} \\ &s.t. \;\; \mathbf{w}^H \mathbf{v}(\theta_d, \phi_d) = 1 \end{aligned}$$

where matrix $\mathbf{A} = \sum_{(\theta_i,\phi_i)\in\Omega} \mathbf{v}(\theta_i, \phi_i)\mathbf{v}^H(\theta_i, \phi_i)$ emulates the covariance matrix of a scenario with a dense set of interference signals uniformly distributed in the sidelobe region (being in our case the region covered by $0 \leq \theta \leq 7.5^\circ$ and $0 \leq \phi \leq 360^\circ$). In practice, this matrix is constructed by uniformly dividing the region of interest in T points. Nonetheless, we have observed in our experiments that good performance results can be obtained by selecting the identity matrix instead of matrix $\mathbf{A}$ and, by doing so, the complexity of the method is considerably reduced. It is worth noting that an additional constraint was included in the original algorithm [7] in order to assure that the maximum gain is obtained in the desired direction. However, our experiments revealed that this constraint is not needed in the considered planar array. Besides, performance is improved as two degrees of freedom are saved.

The initialization step is a constrained optimization problem with the objective of assuring a distortionless response for the desired signal and the minimization of all the directions coming from the sidelobe region Ω. Therefore, the solution can be easily obtained by means of the Lagrangian method as follows:

$$\mathbf{w}^H = \frac{\mathbf{v}^H(\theta_d, \phi_d)\mathbf{A}^{-1}}{\mathbf{v}^H(\theta_d, \phi_d)\mathbf{A}^{-1}\mathbf{v}(\theta_d, \phi_d)}$$

However, this solution does not necessarily imply a response level equal to ε in the sidelobe region. For that reason, additional iterations are included in the algorithm in order to attain the desired response. More specifically, the beamformer is updated at each iteration as follows:

$$\mathbf{w} = \mathbf{w} + \Delta\mathbf{w}$$

where $\Delta\mathbf{w}$ is the solution to the following problem:

$$\begin{aligned} &\min_{\mathbf{w}} \Delta\mathbf{w}^H \mathbf{A} \Delta\mathbf{w} \\ &s.t. \;\; \Delta\mathbf{w}^H \mathbf{v}(\theta_d, \phi_d) = 0 \\ &\qquad \Delta\mathbf{w}^H \mathbf{v}(\theta_j, \phi_j) = f_j \qquad \text{for } j = 1..M-1 \end{aligned}$$

The above constraints are imposed to assure that the distortionless property is maintained ($(\mathbf{w} + \Delta\mathbf{w})^H \mathbf{v}(\theta_d, \phi_d) = 1$ if $\Delta\mathbf{w}^H \mathbf{v}(\theta_d, \phi_d) = 0$) and that the directions in the region Ω with the highest response ($\mathbf{v}(\theta_j, \phi_j) = f_j,\ j = 1..M-1$) attain the desired response (f_j is computed as $f_j = (\varepsilon - |c_j|)c_j/|c_j|$, being c_j the response to the previous beamformer $\mathbf{w}^H \mathbf{v}(\theta_j, \phi_j) = c_j$). By defining matrix

$$\mathbf{C} = [\mathbf{v}(\theta_d, \phi_d), \mathbf{v}(\theta_1, \phi_1), ..., \mathbf{v}(\theta_{M-1}, \phi_{M-1})]$$

and vector $\mathbf{g} = [0, f_1, ..., f_{M-1}]^T$, the following solution is obtained for $\Delta\mathbf{w}$:

$$\Delta\mathbf{w}^H = \mathbf{g}^H \left(\mathbf{C}^H \mathbf{A}^{-1} \mathbf{C}\right)^{-1} \mathbf{C}^H \mathbf{A}^{-1}$$

With the obtained result, the beamforming vector is updated and the algorithm is iterated until convergence. In situations where convergence is attained, the number of required iterations depends on the target pattern response but it is usually of the order of the number of antennas.

It is worth recalling that this is a deterministic beamformer. Then, the beamforming solution for the different LOSS DOAs can be computed off-line and saved.

B. EIG: Adaptive Beamformer with Eigenconstraints

The adaptive beamformer with eigenconstraints (EIG) is designed based on the standard LCMV beamformer [4]. We will introduce besides the distortionless constraint further constraints in order to attenuate as much as possible the region of below 7.5° of elevation, as all the multipath signals and interference signals are expected below 7.5° elevation with respect to the local horizon. The general formulation for a LCMV beamformer is

$$\mathbf{w}_{opt}^H = \mathbf{g}^H \left(\mathbf{C}^H \hat{\mathbf{R}}_{x,pre}^{-1} \mathbf{C}\right)^{-1} \mathbf{C}^H \hat{\mathbf{R}}_{x,pre}^{-1}$$

with the constraints

$$\mathbf{C}^H \mathbf{w} = \mathbf{g}$$

Notice that here we consider the pre-correlation covariance matrix estimate, $\hat{\mathbf{R}}_{x,pre}$, i.e., an estimate of the interference-plus-noise spatial covariance matrix. This is because both the LOSS and multipath signals are quite weak at the pre-correlation samples. Then, the problem of coherent signals is alleviated. On the other hand, $\mathbf{g} = [1\ 0\ \cdots 0]^T$ to introduce the distortionless constraint:

$$\mathbf{w}^H \mathbf{v}(\theta_d, \phi_d) = 1$$

and several null constraints to suppress all signals arriving from lower than 7.5° of elevation. In order to effectively control the beam pattern over a region of azimuth and elevation space we use the so-called eigenvector constraints [4]. These eigenvector constraints will form our null constraints in the general description of LCMV. In order to derive the constraints we define the correlation matrix of the array

$$\mathbf{Q} = \int_\Phi \int_\Theta \mathbf{v}(\theta, \phi)\mathbf{v}^H(\theta, \phi)\, d\theta d\phi$$

where Φ and Θ denote the constraint region of ϕ and θ, respectively. Note that $\mathbf{Q}$ does not depend on the desired pattern shape, but only on the constraint region and the array manifold. Thus, $\mathbf{Q}$ can be calculated in advance and is an input to the adaptive EIG beamformer. Then we define

$$\bar{\mathbf{Q}} = \mathbf{P}_{x,pre}^{\perp}\, \mathbf{Q}\, \mathbf{P}_{x,pre}^{\perp}$$

where $\mathbf{P}_{x,pre}^{\perp} = \mathbf{I} - \mathbf{U}_{x,pre}(\mathbf{U}_{x,pre}^H \mathbf{U}_{x,pre})^{-1}\mathbf{U}_{x,pre}^H$ and $\mathbf{U}_{x,pre}$ denotes the eigenvectors of the principle eigenvalues

of $\mathbf{R}_{x,pre}$. For interference sources with large power we can also write

$$\bar{\mathbf{Q}} = \mathbf{P}^{\perp}_{x,pre}\ \mathbf{Q}\ \mathbf{P}^{\perp}_{x,pre} \approx \hat{\mathbf{R}}^{-1}_{x,pre}\ \mathbf{Q}\ \hat{\mathbf{R}}^{-1}_{x,pre}$$

as it can be shown that $\mathbf{P}^{\perp}_{x,pre} \approx \hat{\mathbf{R}}^{-1}_{x,pre}$ for large interference sources with large power. In other words, for the case that the principle eigenvectors of $\mathbf{R}_{x,pre}$ are large. The eigendecomposition of $\bar{\mathbf{Q}}$ can be written as

$$\bar{\mathbf{Q}} = \mathbf{U}_{\bar{\mathbf{Q}}}\ \mathbf{\Lambda}_{\bar{\mathbf{Q}}}\ \mathbf{U}^{H}_{\bar{\mathbf{Q}}} = \sum_{i=1}^{M} \lambda_i \mathbf{\Phi}_i \mathbf{\Phi}_i^H$$

The matrix $\mathbf{U}_{\bar{\mathbf{Q}}} \in \mathbb{C}^{M\times M}$ is the matrix gathering the eigenvectors,

$$\mathbf{U}_{\bar{\mathbf{Q}}} = [\mathbf{\Phi}_1\ \mathbf{\Phi}_2\ \cdots \mathbf{\Phi}_M]$$

and

$$\mathbf{\Lambda}_{\bar{Q}} = \mathrm{diag}\{\lambda_1\ \lambda_2\ \cdots \lambda_M\}$$

is a diagonal matrix of the ordered eigenvalues. We impose M_e linear constraints on $\mathbf{w}$, $\mathbf{\Phi}_i^H \mathbf{w} = 0 \quad i = 1, \ldots, M_e$.

Normally one chooses M_e to correspond to the number of significant eigenvalues of $\bar{\mathbf{Q}}$. As we increase M_e, we reduce the number of degrees of freedom available for adaptation of the beamformer to the scenario. We choose M_e such that we consider all eigenvectors for which the corresponding eigenvalues are larger than 10% with respect to the maximum eigenvalue. This turned out to be a reasonable trade-off between attenuation of signals arriving from low elevations and number of available degrees of freedom for adaptation.

C. IAA: Iterative Adaptive Algorithm

The Iterative Adaptive Approach (IAA) method is an adaptive beamformer based on a robust design criterion. This algorithm was selected due to its good behavior in terms of robustness as reported in [5]. More specifically, the authors in [5] compared the IAA beamformer with other robust approaches and showed that this option is the most equilibrated strategy in terms of SINR, estimation accuracy of DOA and power of the desired signal.

Further details of the algorithm can be found in [5] but basically the idea consists in defining a scanning grid of L directions by constructing a set of L steering vectors $\mathbf{V} = [\mathbf{v}(\theta_1, \phi_1), ..., \mathbf{v}(\theta_L, \phi_L)]$. Once this scanning grid is defined, the algorithm estimates the powers at each direction and gathers them in matrix $\hat{\mathbf{P}} = diag\{\hat{P}_1, ..., \hat{P}_L\}$. After that, the beamformer for each direction l (with a potential source) is computed as:

$$\mathbf{w}_l^H = \frac{\mathbf{v}^H(\theta_l, \phi_l)\bar{\mathbf{R}}^{-1}}{\mathbf{v}^H(\theta_l, \phi_l)\bar{\mathbf{R}}^{-1}\mathbf{v}(\theta_l, \phi_l)}$$

where $\bar{\mathbf{R}}$ is a estimate of the covariance matrix iteratively computed by considering the received signal $\mathbf{x}(n)$ for N snapshots as follows:

$$\hat{s}_l(n) = \mathbf{v}^H(\theta_l, \phi_l)\mathbf{x}(n)/M \qquad n = 1..N; l = 1..L$$

$$\hat{P}_l = \frac{1}{N}\sum_{n=1}^{N} |\hat{s}_l(n)|^2 \qquad l = 1..L$$

repeat

$\bar{\mathbf{R}} = \mathbf{V}\hat{\mathbf{P}}\mathbf{V}^H$

for $l = 1..L$

$$\mathbf{w}_l^H = \frac{\mathbf{v}^H(\theta_l, \phi_l)\bar{\mathbf{R}}^{-1}}{\mathbf{v}^H(\theta_l, \phi_l)\bar{\mathbf{R}}^{-1}\mathbf{v}(\theta_l, \phi_l)}$$

$\hat{P}_l = \mathbf{w}_l^H \hat{\mathbf{R}}_x \mathbf{w}_l$

end

until convergence

Notice that the beamforming solution is similar to the MPDR approach and the robustness against array perturbations and coherent signals comes from two facts: 1) matrix $\hat{\mathbf{P}}$ is defined by considering that the sources are uncorrelated, and 2) the covariance matrix is estimated by taking into account the power arriving from the directions where the different beamformers are pointing, being this power estimate performed by taking into account the sample covariance matrix $\hat{\mathbf{R}}_x$ (in this case we test IAA for both the pre- and post-correlation cases).

IV. Simulation Results

In this work, we consider an environment with four multipath components and two interference sources with the following parameters:

- Multipath powers modeled as Gamma r.v. with m=30 and average LOSS signal-to-multipath ratio equal to:
  - o SMR_1=9dB, SMR_2=6dB, SMR_3=6dB, SMR_4=9dB.
- Multipath phases modeled as uniform r.v. between -pandp.
- Multipath delays equal to:
  - o T_{MP_1}=0.25ns, T_{MP_2}=0.5ns, T_{MP_3}=0.75ns, T_{MP_4}=1ns.
- In-band interference sources with bandwidth equal to 1 MHz and power equal to P_{i1}=-115 dBW and P_{i2}=-110dBW.

Besides, we also consider four different scenarios in accordance with the DOAs of the LOSS, multipath and interference signals (as presented in Table I). In particular, we consider two groups of scenarios. In the first group (scenarios 1 and 2), LOSS is at 10° elevation, whereas 90° elevation is considered for the second group (scenarios 3 and 4). Clearly, we are considering two representative cases (broadside and close to endfire) to show the properties of the proposed strategies. Concerning the nature of multipath and interference components, two different environments are adopted as well: only multipath environment (scenarios 1 and 3) and multipath-plus-interference environment (scenarios 2 and 4).

Before presenting results obtained with the different strategies, we introduce some figures related with the behaviour of

TABLE I
SIMULATION SCENARIOS.

	LOSS	Multipath	Interference
Scenario 1	θ=10°,ϕ=90°	θ_1=7.5°,ϕ_1=90° θ_2=7.5°,ϕ_2=45° θ_3=7.5°,ϕ_3=135° θ_4=1°,ϕ_4=90°	None
Scenario 2	θ=10°,ϕ=90°	θ_1=7.5°,ϕ_1=90° θ_2=7.5°,ϕ_2=45° θ_3=7.5°,ϕ_3=135° θ_4=1°,ϕ_4=90°	θ_1=7.5°,ϕ_1=135° θ_2=1°,ϕ_2=90°
Scenario 3	θ=90°,ϕ=90°	θ_1=7.5°,ϕ_1=90° θ_2=7.5°,ϕ_2=45° θ_3=7.5°,ϕ_3=135° θ_4=1°,ϕ_4=90°	None
Scenario 4	θ = 90°,ϕ=90°	θ_1=7.5°,ϕ_1 = 90° θ_2=7.5°,ϕ_2=45° θ_3=7.5°,ϕ_3=135° θ_4=1°,ϕ_4=90°	θ_1=7.5°,ϕ_1=135° θ_2=1°,ϕ_2=90°

the beamforming response of the proposed solutions. In Figure 2, we present the beamforming response of the DET approach when it is designed for scenarios 3 and 4 (i.e., when LOSS elevation is 90). For the sake of comparison, we also present the response of the well-known Dolph-Chebychev solution. As observed in the bottom of the figure, the Dolph-Chebychev approach assures that all the sidelobe levels (50 dB in this case) have the same attenuation level but this is achieved at the expense of array gain (approximately 15 dBi are obtained). By considering the DET solution, one can balance the trade-off array gain vs. attenuation. By selection an attenuation level of 50 dB for the multipath+interference region (the same level as Dolph-Chebychev), we can obtain an array gain of 5 dB higher than the other solution (most of the theoretical bound $10\log_{10} 36$ dB + antenna gain at broadside). Therefore, the DET approach offers us a high flexibility to tailor the beam pattern to the scenario considered in the project.

Concerning the adaptive arrays, some problems are found when such kind of techniques are applied in scenarios with coherence signals. In this work we try to circumvent that with two different strategies. In the EIG case, the strategy is based on considering the pre-correlation covariance matrix in order to exploit the fact that LOSS and multipath components are quite weak at that level and LOSS DOA is known. The multipath contribution is then cancelled by nulling the region where these components come from. This is observed in Figure 3, where a polar representation of the EIG beamresponse is presented. As clearly observed, the beamresponse at lower elevations are efficiently cancelled. The second strategy is based on the use of the robust IAA criterion. As commented in the previous section, the algorithm presents a robust behaviour as an estimated version of the covariance matrix is adopted to circumvent coherence signals effects. In order to illustrate the robust behaviour of IAA, we compare results obtained in scenario 3 with those obtained with MPDR in Figure 4 (LOSS azimuth is considered in the figure). As observed, both solutions provide distortionless response at look-direction, DOA of the LOSS. A different behavior is observed at lower elevations due to the presence of multipath components. In the IAA case, these components are efficiently cancelled with 70 dB of attenuation. In other words, IAA is a robust beamfomer against multipath components. MPDR, on the other hand, provides a

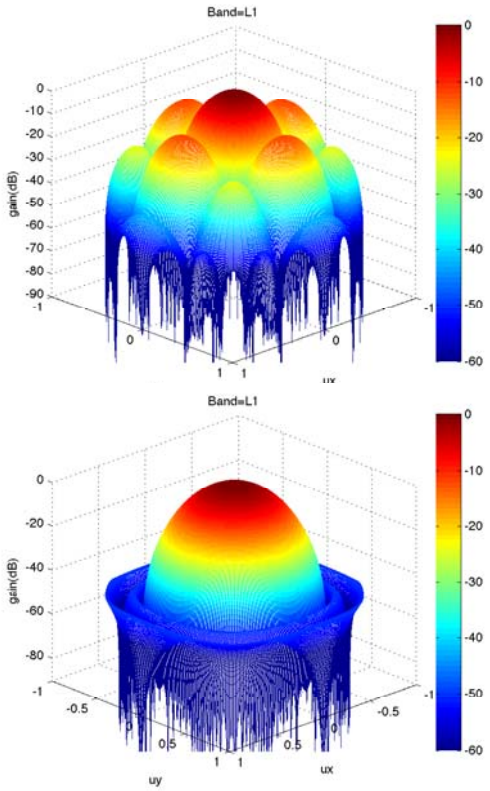

Fig. 2. DET vs. Dolph-Chebychev comparison.

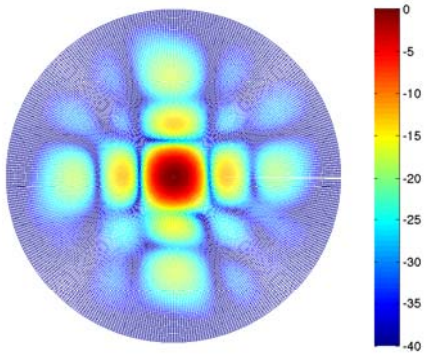

Fig. 3. Polar representation of the EIG beamresponse (scenario 2).

significantly degraded response as the algorithm emphasizes multipath components. As previously explained, this behavior comes from the fact that MPDR tries to compensate the LOSS with the multipath signals with the aim of minimizing total output power.

We conclude this section by presenting Galileo receiver performance. More specifically, we compare the different solutions in terms of DLL and PLL errors. We have also included results for the single antenna (SA) case for benchmarking. In Table II, DLL errors for the L1 band are presented. As observed, the use of digital beamforming allows for a significant error reduction when compared to the antenna case. It is only in scenario 1 where the DET beamformer shows a similar behavior to that observed in the single antenna scheme. This is because the DOAs of the multipath signals are quite close to the DOA of the LOSS component and

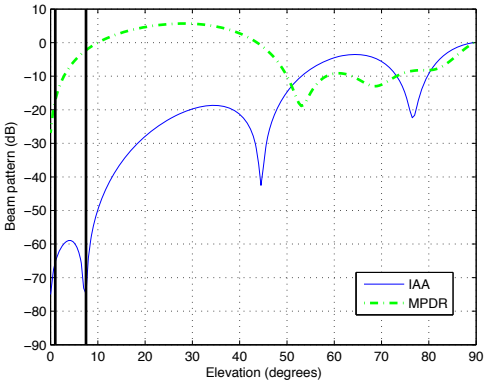

Fig. 4. IAA vs. MPDR (Capon beamformer) comparison (scenario 3).

the beampattern is significantly degraded (poor array gain) when attenuations are forced in the multipath region. In the other scenarios, however, performance of DET beamformer is significantly better. In scenario 2, DET is able of efficiently cancelling the interference components (errors is reduced from 203 cm to 48 cm). In scenarios 3 and 4, the sidelobe levels of the DET solution can be further reduced while providing a good array gain as the LOSS signal is at the broadside. As for the other beamforming techniques, performance is substantially improved in all the cases. In particular, the IAA (pre-correlation version) provides the best results in scenarios 1 and 2, whereas the lowest errors in scenarios 3 and 4 are obtained when the EIG solution is taken into account. The reason why the pre-correlation version of IAA offers a better behavior than its post-correlation counterpart mainly comes from the fact that the distortion of the beam pattern is lower in the first case. Although the IAA beamformer is quite robust to coherence signals, the pattern should be adapted to provide low attenuation levels. As a consequence, a lower array gain is obtained. The deep of these attenuations depends on the power of the multipath signals and, for that reason, better performance is obtained by considering the pre-correlation covariance matrix. Finally, it is worth noting the dependency of EIG behaviour on LOSS elevation. This solution is based on suppressing the whole multipath region. The efficiency of such suppression is higher as so it is the LOSS elevation. For that reason, EIG provides excellent results in Scenarios 3 and 4, whereas poor performance is achieved in the other two environments; specially in the DLL errors case where performance is quite sensitive to array gain degradation. In Table III, results corresponding to the PLL errors are presented. In this case, it is observed a higher digital beamforming gain when comparing the proposed solutions with the single antenna approach. The effect of noise on PLL errors is lower than in the previous case and. For that reason, the impact of array gain losses due to beampattern deterioration is more moderate here. By collecting results obtained in the DLL and PLL cases, one can conclude that errors can be reduced with percentages ranging from 47% to 97% when the pre-correlation version of IAA is adopted.

In Tables II and III, we also show DLL and PLL results associated to E5b. Similar conclusions can be obtained here. However, it is observed that some beamformers obtain worse

TABLE II
DLL ERRORS (EXPRESSED IN CM).

	SA	DET	EIG	IAA (post)	IAA (pre)
Scenario 1 (L1)	38	38	26	17	6.2
Scenario 2 (L1)	203	48	26	18	7.1
Scenario 3 (L1)	8.3	1.5	1.3	2.9	1.4
Scenario 4 (L1)	41	1.9	1.3	2.7	1.5
Scenario 1 (E5b)	11	18	12.3	16.7	3.3
Scenario 2 (E5b)	32	22	12.5	14	3.7
Scenario 3 (E5b)	3	6.4	0.7	3.7	0.7
Scenario 4 (E5b)	8.6	8.9	0.7	3.4	0.7

TABLE III
PLL ERRORS (EXPRESSED IN MM).

	SA	DET	EIG	IAA (post)	IAA (pre)
Scenario 1 (L1)	12.3	6.6	6.1	6	6.5
Scenario 2 (L1)	16.1	6.7	5.6	5.7	5.9
Scenario 3 (L1)	2.7	0.1	0.1	0.1	0.1
Scenario 4 (L1)	3.3	0.1	0.1	0.1	0.1
Scenario 1 (E5b)	18.4	9	10.4	9.6	8.2
Scenario 2 (E5b)	18.5	9.3	8.2	8.6	8
Scenario 3 (E5b)	4	0.3	0.2	1	0.3
Scenario 4 (E5b)	4.8	0.3	0.2	0.9	0.3

results than the single antenna approach in some cases. This is because distance between antenna elements is equal to $\lambda_{L1}/2$. In other words, the separation between antennas is lower than $\lambda_{E5b}/2$ and, for that reason, the beamformer has an increase difficulty to attain good results (the lower the distance, the lower the performance of the beamformer). Nonetheless, the pre-correlation version of the IAA beamformer achieves satisfactory results as tracking errors can be reduced at least 53% (up to 93% in some cases).

V. CONCLUSION

In this paper, we have proposed robust beamforming techniques aimed at mitigating multipath and interference signals. More specifically, one deterministic and two adaptive beamforming strategies adapted to the considered scenario have been considered. The proposed solutions have been validated in different scenarios and compared with the single antenna scheme, showing that tracking errors can be reduced with percentages ranging from 47% to 97%.

REFERENCES

[1] F. Amarillo, A. Ballereau, M. Crisci, B. Lobert, and S. Lannelongue, "Galileo IOV ground mission segment performances," *in Proc. GNSS ENC*, 2008.

[2] G. Seco-Granados, J. A. Fernandez-Rubio, and C. Fernandez-Prades, "Ml estimator and hybrid beamformer for multipath and interference mitigation in gnss receivers," *IEEE Trans. on Signal Processing*, vol. 53, pp. 1194–1208, March 2005.

[3] S. Backen, D. Akos, and M.L. Nordenvaad, "Post-processing dynamic GNSS antenna array calibration and deterministic beamforming," *in Proc. of the 21st International Technical Meeting of the Satellite Division of the ION (ION GNSS 2008), Savannah*, 2008.

[4] H.L. Van Trees, *Optimum Array Processing (Detection, Estimation and Modulation Theory, Part IV)*, John Wiley, 2002.

[5] L. Du, T. Yardibi, J. Li, and P. Stoica, "Review of user parameter-free robust adaptive beamforming algorithms," *Digital Signal Processing*, vol. 19, pp. 567–582, 2009.

[6] T. N. Morrissey, K. W. Shallberg, A. J. Van Dierendonck, and M. J. Nicholson, "GPS receiver performance characterization under realistic ionospheric phase scintillation environments," *Radio Science*, vol. 39, 2004.

[7] C-Y. Tseng and L. J. Griffiths, "A simple algorithm to achieve desired patterns for arbitrary arrays," *IEEE Trans. on Signal Processing*, vol. 40, pp. 2737–2746, Nov. 1992.